# Resonant inelastic x-ray scattering studies of elementary excitations

Ament, L.J.P.

# Chapter 3

# Charge excitations

## 3.1 Introduction

Charge excitations occur at quite high energies (typically, the gap of Mott insulators is of the order of a few eV), which placed them within reach of RIXS experiments already in the early stages of the development of the technique. Charge excitations, both charge transfer excitations and exctitations across the Mott gap [22], are interesting by themselves, but also because the high energy theory that describes them contains the low energy physics as well. The latter are of interest when one studies the elementary magnetic and orbital excitations of the solid.

Other questions that can be addressed with RIXS relate to the nature of the charge excitations – whether or not they form bound exciton states, if these propagate coherently, etc. [3].

In this chapter, we study the indirect RIXS response of Hubbard models. The simplest case of a single band Hubbard model with spinless fermions yields a RIXS spectrum proportional to the dynamic charge correlation function $S(\mathbf{q}, \omega)$. This model is of interest in, *e.g.*, doped cuprates, since the Coulomb repulsion is so large that doubly occupied sites only virtually form. The spin degree of freedom is, to first order, irrelevant for the charge excitations in these systems. Introducing spin or multiple bands complicates this picture somewhat, and yields less simple correlation functions. The work in Sec. 3.2 is published in Phys. Rev. B. We present some extensions of that work after fruitful discussions with Y.-J. Kim, describing in more detail the difference between the well and poorly screened intermediate states. The experimental results of Y.-J. Kim are reviewed at the end

of this chapter. In Sec. 3.3, the first order corrections to the charge scattering cross section for strong core hole potentials are presented, which yield information about the hopping amplitudes. Sec. 3.4 contains an analysis of the polarization dependence of transition metal K edge RIXS.

## 3.2 UCL approach to charge scattering

Published as '*Ultrashort Lifetime Expansion for Indirect Resonant Inelastic X-ray Scattering*' in Phys. Rev. B **75**, 115118 (2007) with Fiona Forte and Jeroen van den Brink.

**Abstract.** *In indirect resonant inelastic X-ray scattering (RIXS) an intermediate state is created with a core hole that has an ultra-short lifetime. The core hole potential therefore acts as a femtosecond pulse on the valence electrons. We show that this fact can be exploited to integrate out the intermediate states from the expressions for the scattering cross section. By doing so we obtain an effective scattering cross section that only contains the initial and final scattering states. This effective cross section which turns out to be a resonant scattering factor times a linear combination of the charge response function $S(\mathbf{q},\omega)$ and the dynamic longitudinal spin density correlation function, both with a resonant prefactor. This result is asymptotically exact for both strong and weak local core hole potentials and ultra-short lifetimes. The resonant scattering pre-factor is shown to be weakly temperature dependent. We also derive a sum rule for the total scattering intensity and generalize the results to multi-band systems. One of the remarkable outcomes is that one can change the relative charge and spin contribution to the inelastic spectral weight by varying the incident photon energy.*

### 3.2.1 Introduction

It is a well-known fact that the 1s core hole that is created in indirect RIXS has an ultra-short lifetime, of the order of femtoseconds. The reason is that the core hole has a very high energy and is prone to decay via all sorts of radiative and non-radiative processes, severely cutting down the efficiency of RIXS. In the canonical theoretical treatments of RIXS this lifetime effect is normally introduced as a core hole broadening and disregarded from that point on.

In a previous study [49], however, we have shown that from the theory perspective there is a great advantage to the extremely short lifetime of the core hole. The ultra-short lifetime implies that for the electrons in the solid –particularly for the slow ones that are close to the Fermi-energy– the core hole potential is almost an instantaneous delta-function in time. Although the core hole potential by itself can be large and therefore a strong perturbation to the electrons, the very short duration of this perturbing potential allows for a systematic expansion of the scattering cross section in terms of the core hole lifetime. Here we

present a detailed derivation and various generalizations of this result. We shall see that the most important consequence of the ultra-short core hole lifetime is that for indirect RIXS the effective scattering cross section is proportional to the charge structurefactor $S(\mathbf{q},\omega)$ and the longitudinal spin structure factor that is associated with it.

The indirect RIXS process is shown schematically in Fig. 1.2. In transition metal systems the photo-electron is promoted from a 1s core orbital to empty 4p states that are far (10-20 eV) above the Fermi level. So the X-rays do not cause direct transitions of the 1s electron into the lowest 3d-like conduction bands of the system. Still RIXS is sensitive to excitations of electrons near the Fermi level. The Coulomb potential of 1s core hole causes, *e.g.*, very low energy electron-hole excitations in the conduction/valence band: the core hole potential is screened by the valence electrons. When the excited 4p electron recombines with the 1s core hole and the outgoing photon is emitted, the system can therefore be left behind in an excited final state. Since the excitations are caused by the core hole, we refer to this scattering mechanism as *indirect* RIXS.

In this chapter, we derive in detail the dynamical correlation function that is measured in indirect RIXS. We aim to give a full and self-contained derivation of the results that were presented earlier [49] and we elaborate on several generalizations. In particular we will show that for local core hole potentials and ultra-short lifetimes, the dynamical correlation function is a linear combination of the charge density and longitudinal spin density response function. For a single band system the actual linear combination that is measured depends on the energy of the incoming photons and we determine the precise energy dependence of its coefficients. A sum rule is derived and we generalize these results to the case of finite temperature and for multi-band systems.

### 3.2.2 Series expansion of the scattering cross section

The Kramers-Heisenberg formula [33, 41, 42, 55] for the resonant X-ray scattering cross section at finite temperature is given by Eq. (2.32). In the following we will take the groundstate energy of our system as reference energy for the electronic system: $E_g \equiv 0$. We define the resonance energy $\hbar\omega_{\rm res}$ to be somewhere in the middle of the resonant edge: it is just a number serving as a reference energy in the intermediate state. The energy of the incoming X-rays with respect to the resonance energy is $\hbar\omega_{\rm in}$ (this energy can thus either be negative or positive: $\omega_{\rm in} = \omega_{\mathbf{k}} - \omega_{\rm res}$) and in the following, $E_n$ is the energy of intermediate state $|n\rangle$ with respect to the resonance energy. In the intermediate state a core hole and a photo-excited electron are present. When we take the Coulomb interaction between the intermediate state core hole and the valence band electrons into account, we obtain a finite inelastic scattering amplitude. In that case there is a non-zero probability that an electron-hole excitation is present in the final state, see Fig. 1.2.

Crucial to our further considerations will be the fact that the intermediate

state is not a steady state. The reason is that the highly energetic 1s core hole quickly decays, *e.g.*, via Auger processes, and the core hole lifetime is very short. The Heisenberg time-energy uncertainty relationship then implies that the core hole energy has an appreciable uncertainty. This uncertainty appears in the formalism above as the core hole energy broadening $\Gamma$ which is proportional to the inverse core hole lifetime, which is of the order of electronvolts as the lifetime is ultra-short, of the order of femtoseconds. Note that the lifetime broadening only appears in the intermediate states and not in the final or initial states –these both have very long lifetimes. This implies that the core hole broadening does not present an intrinsic limit to the experimental resolution of RIXS: the loss energy $\omega$ is completely determined by kinematics.

When the incoming energy of the X-rays is equal to a resonant energy of the system $\hbar\omega_{\text{in}} - E_n = 0$ and we see from Eqs. (2.30) and (2.31) that the resonant enhancement of the X-ray scattering cross section is $(\hbar\omega_{\text{res}}/\Gamma)^2$, which is $\sim 10^6$ for a transition metal K edge [33].

In a resonant scattering process, the measured system is generally strongly perturbed. Formally this is clear from the Kramers-Heisenberg formula (2.31), in which both the energy and the wavefunction of the intermediate state –where a potentially strongly perturbing core hole is present– appear. This is in contrast with canonical optical/electron energy loss experiments, where the probing photon/electron presents a weak perturbation to the system that is to be measured.

To calculate RIXS amplitudes, one possibility is to numerically evaluate the Kramers-Heisenberg expression. To do so, all initial, intermediate and final state energies and wavefunctions need to be known exactly, so that in practice a direct evaluation is only possible for systems that, for example, consist of a small cluster of atoms [56,57]. In this chapter, however, we show that under the appropriate conditions we can integrate out the intermediate states from the Kramers-Heisenberg expression. After doing so, we can directly relate RIXS amplitudes to linear charge and spin response functions of the unperturbed system. For non-resonant scattering, one is familiar with the situation that the scattering intensity is proportional to a linear response function, but for a resonant scattering experiment this is a quite unexpected result.

Let us proceed by formally expanding the scattering amplitude in a power series, following Eq. (2.49):

$$\mathcal{F}_{fg} = \frac{1}{\hbar\omega_{\text{in}} + i\Gamma} \sum_{l=0}^{\infty} M_l, \tag{3.1}$$

where we introduced the matrix elements

$$M_l = \sum_n \left( \frac{E_n}{\hbar\omega_{\text{in}} + i\Gamma} \right)^l \langle f| \mathcal{D}^\dagger |n\rangle \langle n| \mathcal{D} |g\rangle . \tag{3.2}$$

The formal radius of convergence of this power series is given by $E_n^2/[(\hbar\omega_{\text{in}})^2+\Gamma^2]$, so that the series is obviously convergent when the incoming X-ray energy is, *e.g.*,

far enough below the resonance, *i.e.*, when $|\omega_{\text{in}}| \gg 0$. But also at resonance, when $\omega_{\text{in}} = 0$ the series is convergent for intermediate energies that are smaller than the core hole broadening $\Gamma$. Thus this expansion is controlled for ultra-short core hole lifetimes, which implies that $\Gamma$ is large. In the following we will be performing resummations of this series.

We denote the denominator of the expansion parameter $\hbar\omega_{\text{in}} + i\Gamma$ by the complex number $\Delta$, so that

$$M_l = \frac{1}{\Delta^l} \sum_n \langle f| \mathcal{D}^\dagger |n\rangle (E_n)^l \langle n| \mathcal{D} |i\rangle = \frac{1}{\Delta^l} \langle f| \mathcal{D}^\dagger (H_{\text{int}})^l \mathcal{D} |i\rangle , \tag{3.3}$$

where $H_{\text{int}}$ is the Hamiltonian in the intermediate state. We thus obtain the following series expansion for the resonant cross section:

$$\left.\frac{d^2\sigma}{d\omega d\Omega}\right|_{res} \propto \left\langle \sum_f \left| \frac{1}{\Delta} \sum_{l=0}^{\infty} M_l \right|^2 \delta(\omega - \omega_{fi}) \right\rangle_{\text{T}} \tag{3.4}$$

where $\langle \dots \rangle_T$ denotes a thermal average and $\hbar\omega_{fi}$ is the energy gained by the material.

### 3.2.3 Indirect RIXS for spinless fermions: $T = 0$

As in Ref. [49], we will first calculate the resonant X-ray cross section at zero temperature in the case where the valence and conduction electrons are effectively described by a single band of spinless fermions: spin and orbital degrees of freedom of the valence electron system are suppressed. Physically this situation can be realized in a fully saturated ferromagnet.

The final and initial states of the system are determined by a Hamiltonian $H_0$ that describes the electrons around the Fermi level. The generic form of the full many-body Hamiltonian is

$$H_0 = \sum_{i,j} t_{ij}(c_i^\dagger c_j + c_j^\dagger c_i) + c_i^\dagger c_i V_{ij} c_j^\dagger c_j, \tag{3.5}$$

where $i$ and $j$ denote lattice sites with lattice vectors $\mathbf{R}_i$ and $\mathbf{R}_j$. Note that the sum is over each pair $i, j$ once, with $i, j$ ranging from 1 to $N$, where $N$ is the number of sites in the system. The hopping amplitudes of the valence electrons are denoted by $t_{ij}$ and the $c/c^\dagger$-operators annihilate/create such electrons. The Coulomb interaction between valence electrons is $V_{ij} = V(|\mathbf{R}_i - \mathbf{R}_j|)$, as the Coulomb interaction only depends on the relative distance between two particles.

The intermediate states are eigenstates of the Hamiltonian $H_{\text{int}} = H_0 + H_c$, where $H_c$ accounts for the Coulomb coupling between the intermediate state core hole and the valence electrons:

$$H_c = \sum_{i,j} s_i s_i^\dagger V_{ij}^c c_j c_j^\dagger, \tag{3.6}$$

where $s_i$ creates a core hole on site $i$. The form of $H_c$ has been chosen such that the well-screened intermediate state is at energy $\hbar\omega_{\rm res}$, so the UCL expansion is around the well-screened part of the absorption edge. We assume that the core hole is fully localized and has no dispersion. We will see shortly that this leads to major simplifications in the theoretical treatment of indirect RIXS. The core hole-valence electron interaction is attractive: $V^c > 0$. An analysis of the polarization dependence is given in Sec. 3.4. For now, we simplify the dipole operators by taking

$$\mathcal{D} = \sum_i e^{-i\mathbf{k}\cdot\mathbf{R}_i} s_i p_i^\dagger + e^{i\mathbf{k}'\cdot\mathbf{R}_i} s_i^\dagger p_i + \text{h.c.}, \tag{3.7}$$

where $p^\dagger$ creates a photo-excited electron in a 4p state and h.c. denotes the hermitian conjugate of both terms.

**Short Lifetime Approximation: Algebraic Form.** In order to calculate the cross section, we need to evaluate the operator $(H_{\rm int})^l = (H_0 + H_c)^l$ in equation (3.3). A direct evaluation of this operator is complicated by the fact that $[H_0, H_c] \neq 0$. We therefore proceed by approximating $H_{\rm int}^l$ with a series that contains the leading terms to the scattering cross section for both strong and weak core hole potentials – as long as the core hole lifetime is short. After that we will do a full resummation of that series. This approximation is central to the results in this chapter.

Expanding $(H_0 + H_c)^l$ gives a series with $2^l$ terms of the form

$$H_{\rm int}^l = H_c^l + \sum_{n=0}^{l-1} H_c^n H_0\, H_c^{l-n-1} + \cdots + \sum_{n=0}^{l-1} H_0^n H_c\, H_0^{l-n-1} + H_0^l. \tag{3.8}$$

Using $H_0\mathcal{D}\,|g\rangle = \mathcal{D}H_0\,|g\rangle \equiv 0$, this series reduces to

$$H_{\rm int}^l \mathcal{D}\,|g\rangle = \left( H_c^l + \sum_{n=0}^{l-2} H_c^n H_0\, H_c^{l-n-1} + \cdots + H_0^{l-1} H_c \right) \mathcal{D}\,|g\rangle\,. \tag{3.9}$$

Using in addition that $\langle f|\,\mathcal{D}^\dagger H_0 = \langle f|\,H_0\mathcal{D}^\dagger = E_f\,\langle f|\,\mathcal{D}^\dagger$, we find

$$\begin{aligned}\langle f|\,\mathcal{D}^\dagger H_{\rm int}^l \mathcal{D}\,|g\rangle = \langle f|\,\mathcal{D}^\dagger \big( H_c^l + E_f\, H_c^{l-1} + \sum_{n=1}^{l-2} H_c^n H_0\, H_c^{l-n-1} \\ + \cdots + E_f^{l-1} H_c \big)\, \mathcal{D}\,|g\rangle\,.\end{aligned} \tag{3.10}$$

For strong core hole potentials, the leading term of $H_{\rm int}^l$ is $H_c^l$. Corrections to this term contain at least one factor of $H_0$ and are therefore smaller by a factor of $t/V^c$. For weak core hole potentials, the leading order term, $H_0^l$, vanishes because $[H_0, \mathcal{D}] = 0$. In this limit, the leading term in the inelastic scattering

amplitude is therefore $E_f^{l-1} H_c$. Correction terms contain at least two factors of $H_c$, which make them at least a factor of $V^c/t$ smaller.

Let us now consider the approximate expression

$$H_{\text{int}}^l \mathcal{D} \left|g\right\rangle \approx \sum_{m=0}^{l} H_0^m H_c^{l-m} \mathcal{D} \left|g\right\rangle . \tag{3.11}$$

From the arguments above, it is easy to see that the leading order terms for both strong ($m = 0$) and weak ($m = l - 1$) core hole potentials are included in the sum; but a large series of other terms are included as well; they can be neglected in the case that we strictly consider either limit. Including them, however, means that we consider in addition a set of higher order scattering processes. A major advantage of including these is that the terms will give rise to a smooth interpolation between the two extreme limits. Note that the $m = l$ term in Eq. (3.11) is 0, so that it can be removed from the sum. After performing the same manipulations as above, we obtain

$$\begin{aligned} \left\langle f\right| \mathcal{D}^\dagger \sum_{m=0}^{l-1} H_0^m H_c^{l-m} \mathcal{D} \left|g\right\rangle &= \sum_{m=0}^{l-1} E_f^m \left\langle f\right| \mathcal{D}^\dagger H_c^{l-m} \mathcal{D} \left|g\right\rangle \\ &= \left\langle f\right| \mathcal{D}^\dagger \left( H_c^l + E_f H_c^{l-1} + \cdots + E_f^{l-1} H_c \right) \mathcal{D} \left|g\right\rangle . \end{aligned} \tag{3.12}$$

Comparing Eqs. (3.10) and (3.12), it can be seen that the approximation (3.11) is exact in the limit of both strong and weak core hole potentials.

**Short Lifetime Approximation: Graphical Representation.** We can also represent the series expansion and its approximation graphically (Fig. 3.1). When we expand $(A+B)^l$, where $A$ and $B$ are non-commuting operators, each term in the series corresponds to a graph on the grid of graph 1. Each graph occurs only once and can be constructed by starting at the lower left corner of the grid and moving either to the right, representing an $A$, or up, representing a $B$. At the next vertex a new move (right or up) is made. We perform this procedure $l$ times and in this way we can obtain $2^l$ distinct graphs, each corresponding to a term in the expansion of $(A+B)^l$. For example moving $l$ times to the right represents the term $A^l$ and moving $l$ times up corresponds to $B^l$, see graphs 2 and 3. All other terms in the series can be constructed by moving up and right a different number of times and in different order. As we consider a fixed value of $l$ ($l = 8$ in Fig. 3.1), all graphs must end on the diagonal of the triangle that forms the grid. In the series for $(H_0+H_c)^l \mathcal{D} \left|g\right\rangle$ ($H_0 = A$ and $H_c = B$) we have the simplification that terms ending with $H_0$ acting on the groundstate give zero. These terms can thus be removed from the expansion. The graphs for this expansion now live on a reduced grid where the horizontal grid-lines at the diagonal of the triangle are absent, see graph 5: these represent all terms ending on $A$.

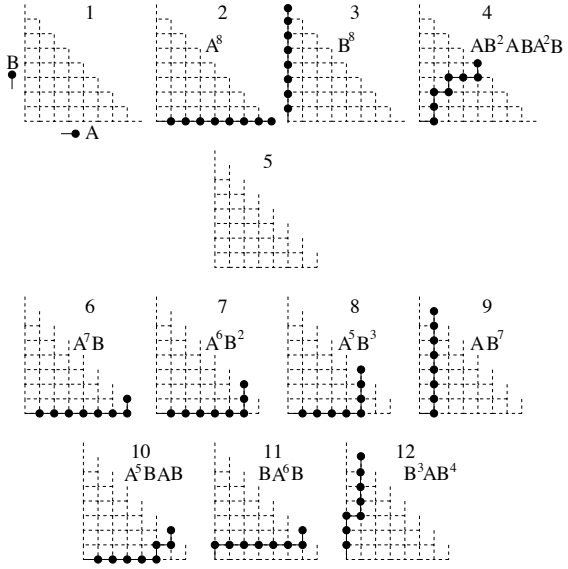


**Figure 3.1:** Graphical representation of the expansion of $(A + B)^l$, where $A = H_0$ and $B = H_c$ are two non-commuting operators. In this example $l = 8$.

In Fig. 3.1 we also represent the approximate series of the right-hand side of Eq. (3.11). Graphically this sum corresponds to the set of graphs on the reduced grid of graph 5, with either one kink (graphs 6-9) or without kinks (graphs 2 and 3). Thus, in our approximation in Eq. (3.11) of the exact series for $(H_0 + H_c)^l$ we neglect all graphs with two or more kinks (graphs 4, 10-12). In the limit of either very $A$ or very large $B$, the graphs that we neglect correspond to sub-leading order corrections. When $A$ is largest, the leading terms are, first, graph 2, which is however zero because it ends on $A$. The leading term is therefore of the order $A^7$ and shown in graph 6. Other higher order terms are shown in the graphs 7, 8, 10 and 11. The last two graphs are neglected in our approximate expansion. In case $B$ is dominating, the leading term is $B^8$, graph 3, and next to leading is graph 9, with $B^7$. The highest order terms that are neglected in our approximate series are of the type shown in graph 12.

**Resummation of Series for Scattering Cross Section.** In order to obtain $M_l$ and from there the scattering amplitude $\mathcal{F}_{fg}$ and finally the scattering cross section, in Eq.(3.12) we need to evaluate expressions of the kind

$$H_c^n \mathcal{D} \, |g\rangle = H_c^{n-1} \sum_{i,l,j} s_l \, s_l^\dagger V_{lj}^c c_j c_j^\dagger e^{-i\mathbf{k}\cdot\mathbf{R}_i} s_i \, p_i^\dagger \, |g\rangle \, . \tag{3.13}$$

In the initial state no core hole is present: just one core hole is created by the dipole operator. We therefore have that $s_l \, s_l^\dagger s_i \, |g\rangle = \delta_{l,i} s_i \, |g\rangle$. Inserting this in

Eq. (3.13), we obtain

$$H_c^n \mathcal{D} \left|g\right\rangle = H_c^{n-1} \sum_i e^{-i\mathbf{k}\cdot\mathbf{R}_i} s_i p_i^\dagger \sum_j V_{ij}^c c_j c_j^\dagger \left|g\right\rangle \tag{3.14}$$

and by recurrence

$$H_c^n \mathcal{D} \left|g\right\rangle = \sum_i e^{-i\mathbf{k}\cdot\mathbf{R}_i} s_i p_i^\dagger \left[\sum_j V_{ij}^c c_j c_j^\dagger\right]^n \left|g\right\rangle . \tag{3.15}$$

Let us for the moment consider the strong core hole potential limit and keep in the expansion Eq. (3.11) only the term $m = 0$. Inserting the results above in Eq. (3.3), we find that

$$M_l = \frac{1}{\Delta^l} \left\langle f\right| \sum_i e^{i\mathbf{q}\cdot\mathbf{R}_i} \left[\sum_j V_{ij}^c c_j c_j^\dagger\right]^l \left|g\right\rangle \quad \text{if} \quad V^c \gg t \tag{3.16}$$

where the transfered momentum $\hbar\mathbf{q} \equiv \hbar\mathbf{k}' - \hbar\mathbf{k}$.

The first important observation is that the term $l = 0$ does not contribute to the inelastic X-ray scattering intensity because $M_0 = \left\langle f\right| \sum_i e^{i\mathbf{q}\cdot\mathbf{R}_i} \left|g\right\rangle = N\delta_{\mathbf{q},\mathbf{0}}\delta_{f,g}$, which only contributes to the elastic scattering intensity at $\mathbf{q} = \mathbf{0}$ (and other multiples of the reciprocal lattice vectors). From inspection of equation (3.2) we see immediately that the $l = 0$ term actually vanishes irrespective of the strength of the core hole potential. This is of relevance when we consider the scattering cross section in the so-called 'fast collision approximation' [58]. This approximation corresponds to the limit where the core hole lifetime broadening is the largest energy scale in system ($\Gamma \to \infty$ or, equivalently, $\mathfrak{Im}\{\Delta\} \to \infty$). In this limit only the $l = 0$ term contributes to the indirect RIXS amplitude and the resonant inelastic signal vanishes. In any theoretical treatment of indirect resonant scattering one therefore needs to go beyond the fast-collision approximation.

This vanishing of spectral weight is ultimately due to an interference effect. If we study a process in which we start from the initial state and reach a certain final state, we need to consider all different possible paths for this excitation–de-excitation process. When the core hole broadening is very large we can reach the final state via any intermediate state and in order to obtain the scattering amplitude we thus add up coherently the contributions of all intermediate states. We then obtain $\mathcal{F} = \sum_n \left\langle f\right| n\rangle \left\langle n\right| g\rangle$. When the set of intermediate states that we sum over is complete (which by definition is the case when $\Gamma \to \infty$ ), this leaves us with $\mathcal{F} = \left\langle f\right| g\rangle$ which is, because of the orthogonality of eigenstates, only non-zero when the initial and final state are equal–hence only when the scattering is elastic. Alternatively, one could say that the scattering process happens so fast that the valence electrons do not have enough time to react: they remain in the ground state.

The second observation is that $M_l$ is a $2^l$-particle correlation function. If we measure far away from resonance, where $|\mathfrak{Re}\{\Delta\}| \gg 0$, the scattering cross section is dominated by the $l = 1$, two-particle, response function. When the incoming photon energy approaches the resonance, gradually the four, six, eight etc. particle response functions add more and more spectral weight to the inelastic scattering amplitude. Generally these multi-particle response functions interfere. We will show, however, that in the local core hole approximation the multi-particle correlation functions in expansion (3.11) collapse onto the dynamic two-particle (charge-charge) and four-particle (spin-spin) correlation function.

**Local core hole potentials.** In hard X-ray electron spectroscopies one often makes the approximation that the core hole potential is local. This corresponds to the widely used Anderson impurity approximation in the theoretical analysis of, *e.g.*, X-ray absorption and photo-emission, introduced in Refs. [59–61]. This approximation is reasonable as the Coulomb potential is certainly largest on the atom where the core hole is located.

In the present case, moreover, we can consider the potential generated by both the localized core hole and photo-excited electron at the same time. As this exciton is a neutral object, its monopole contribution to the potential vanishes for distances larger than the exciton radius. The multi-polar contributions that we are left with in this case are generally small and drop off quickly with distance.

We insert a local core hole potential $V^c_{ij} = U\delta_{ij}$ in our equations and aim to resum the approximate series expansion in Eq. (3.11) for arbitrary values of the local core hole potential. We find from Eq. (3.15) that

$$H^n_c \mathcal{D} \left|g\right\rangle = \sum_i e^{-i\mathbf{k}\cdot\mathbf{R}_i} s_i p^\dagger_i U^n [c_i c^\dagger_i]^n \left|g\right\rangle \tag{3.17}$$

Using that for fermions $[c_i c^\dagger_i]^n = c_i c^\dagger_i$, we obtain for our spinless fermions

$$M^{sf}_l = \frac{1}{\Delta^l} \left\langle f\right| \sum_i e^{i\mathbf{q}\cdot\mathbf{R}_i} c_i c^\dagger_i \left|g\right\rangle \sum_{m=0}^{l-1} E^m_f U^{l-m}. \tag{3.18}$$

The sum over $m$ can easily be performed:

$$\sum_{m=0}^{l-1} E^m_f U^{l-m} = U^l \sum_{m=0}^{l-1} (E_f/U)^m = \frac{U^l - E^l_f}{1 - E_f/U} \tag{3.19}$$

and we obtain for the inelastic part

$$M^{sf}_l = -\frac{1}{\Delta^l} \frac{U^l - E^l_f}{1 - E_f/U} \left\langle f\right| \sum_i e^{i\mathbf{q}\cdot\mathbf{R}_i} c^\dagger_i c_i \left|i\right\rangle. \tag{3.20}$$

Note that $\sum_i e^{i\mathbf{q}\cdot\mathbf{R}_i} c^\dagger_i c_i = \sum_{\mathbf{k}} c^\dagger_{\mathbf{k}-\mathbf{q}} c_{\mathbf{k}} \equiv \rho_{\mathbf{q}}$ is the density operator.

We now have to perform the sum over $l$ in equation (3.1). The $l = 0$ term is zero, as we discussed above, so that the scattering amplitude is

$$\mathcal{F}_{fg} = \frac{1}{\Delta} \sum_{l=1}^{\infty} M_l. \tag{3.21}$$

Using

$$\sum_{l=1}^{\infty} (U/\Delta)^l - (E_f/\Delta)^l = \Delta \frac{U - E_f}{(\Delta - U)(\Delta - E_f)} \tag{3.22}$$

we finally find that the indirect resonant inelastic scattering amplitude for spinless fermions is

$$\mathcal{F}_{fg}^{sf} = P_1(\omega, U) \langle f | \rho_{\mathbf{q}} | g \rangle , \tag{3.23}$$

where the resonant enhancement factor is $P_1(\omega, U) \equiv -U[(\Delta - U)(\Delta - \hbar\omega)]^{-1}$ and $\hbar\omega = E_f$. For spinless fermions with a local core hole potential the scattering cross section thus turns out to be the density response function –a two-particle correlation function– with a resonant prefactor $P_1(\omega)$ that depends on the loss energy $\hbar\omega$, the distance from resonance $\hbar\omega_{\text{in}} (= \mathfrak{Re}\{\Delta\})$, on the core hole potential $U$ and on the core hole lifetime broadening $\Gamma (= -\mathfrak{Im}\{\Delta\})$. We see that the resonant enhancement is largest when the energy of the incoming photons is either equal to the core hole potential ($\hbar\omega_{\text{in}} = U \Rightarrow \hbar\omega_{\mathbf{k}} = \hbar\omega_{\text{res}} + U$) or to the loss energy, which one could refer to as a "final state resonance" ($\hbar\omega_{\text{in}} = \hbar\omega \Rightarrow \hbar\omega_{\mathbf{k}'} = \hbar\omega_{\text{res}}$).

Alternatively, one can perform the UCL expansion at a different intermediate state/$\hbar\omega_{\text{res}}$. Expanding around the poorly screened state by taking

$$H_c = U \sum_i s_i s_i^\dagger c_i^\dagger c_i \tag{3.24}$$

one gets

$$\mathcal{F}_{fg} = P_1(\omega, -U) \langle f | \rho_{\mathbf{q}} | g \rangle . \tag{3.25}$$

Now, $\hbar\omega_{\text{res}}$ refers to the poorly screened state, which is at an energy $U$ above the well-screened state $\hbar\omega_{\text{res}}^{ws}$. Resonance is thus expected when $\hbar\omega_{\text{in}} = -U \Rightarrow \hbar\omega_{\mathbf{k}} = \hbar\omega_{\text{res}}^{ws}$ and $\hbar\omega_{\text{in}} = \hbar\omega \Rightarrow \hbar\omega_{\mathbf{k}'} = \hbar\omega_{\text{res}}^{ws} + U$. This corresponds to energy gain scattering, but that does not occur at low temperatures. Therefore, this resonant behavior cannot be seen in practice.

One then might wonder around which $\hbar\omega_{\text{res}}$ to expand, since the choice of $\hbar\omega_{\text{res}}$ determines the resonant behavior. One way to deal with this problem is simply to take an average of both expansion points. Both resonances are recovered, of which one (the energy-gain resonance) is experimentally inaccessible.

The density response function is related to the dielectric function $\epsilon(\mathbf{q}, \omega)$ and the dynamic structure factor $S(\mathbf{q}, \omega)$ (see, *e.g.*, Ref. [62], p. 322), so that we obtain for the resonant scattering cross section

$$\left.\frac{d^2\sigma}{d\Omega d\omega}\right|_{res}^{sf} \propto -|P_1(\omega)|^2 \, \mathfrak{Im}\left\{\frac{1}{V_{\mathbf{q}}\epsilon(\mathbf{q}, \omega)}\right\} \propto |P_1(\omega)|^2 \, S(\mathbf{q}, \omega), \tag{3.26}$$

for a fixed value of the core hole potential $U$. $V_{\mathbf{q}}$ is the Fourier transform of the Coulomb potential. For weak core hole potentials the total scattering intensity is proportional to $U^2$ and for strong core hole potentials, where $U \gg \Gamma$, the scattering intensity at resonance ($\omega_{\text{in}} = 0$) is to first order independent of the strength of the core hole potential. Far away from the edge, however, where $|\hbar\omega_{\text{in}}| \gg U$, the scattering intensity is again proportional to $U^2$, just as for weak core hole potentials. Integrating $|P_1(\omega)|^2$ over all incoming photon energies, we obtain the integrated inelastic intensity at fixed loss energy $\hbar\omega$ and momentum $\hbar\mathbf{q}$

$$\int_{-\infty}^{\infty} d(\hbar\omega_{\text{in}}) \frac{d^2\sigma}{d\Omega d\omega}\bigg|_{\text{res}}^{sf} = r_e^2 m^2 \omega_{\text{res}}^4 \frac{2\pi U^2}{\Gamma(4\Gamma^2 + (U - \hbar\omega)^2)} S(\mathbf{q}, \omega) \tag{3.27}$$

where we have taken $\omega_{\mathbf{k}^{(\prime)}}$ constant ($= \omega_{\text{res}}$) in the domain of integration: $(-\infty, +\infty)$ implies integration over the energy range described by our theory, *i.e.*, $\sim 10$ eV around the edge. It seems that the resonant enhancement factor of the integrated intensity has a maximum when the loss energy is equal to the core hole potential. However, the core hole potential is attractive and therefore lower than zero, and the loss energy $\hbar\omega$ is by definition greater than zero. So the integrated intensity is maximal at energy loss $\hbar\omega = 0$.

### 3.2.4 Indirect RIXS for spinless fermions: finite $T$

In this section, we generalize the previous calculation to the case of finite temperature. The starting point is Eq. (2.32):

$$\frac{d^2\sigma}{d\Omega d\omega}\bigg|_{\text{res}} \propto \frac{1}{Z} \sum_{i,f} e^{-\beta E_i} |\mathcal{F}_{fi}|^2 \delta(\omega - \omega_{fi}), \tag{3.28}$$

where $Z = \sum_i e^{-\beta E_i}$ is the partition function and $\beta = 1/k_B T$. Eq. (3.28) represents the statistical average over all the initial states $|i\rangle$, where now the more general relation $H_0 |i\rangle = E_i |i\rangle$ holds.

We expand the scattering amplitude $\mathcal{F}_{fi}$, using again the ultra-short lifetime of the core hole as in Eq. (3.1). We are left with the evaluation of the operator $(H_{\text{int}})^l$. We proceed by expanding it in the following way:

$$\begin{aligned}(H_{\text{int}})^l \mathcal{D} |i\rangle &= (H_0 + H_c)^l \mathcal{D} |i\rangle \\ &\approx \sum_{n=0}^{l-1} \sum_{m=0}^{l-n-1} (H_0)^m (H_c)^{l-m-n} (H_0)^n \mathcal{D} |i\rangle \,,\end{aligned} \tag{3.29}$$

where we neglected the term $H_0^l$, as it will not contribute to the inelastic scattering cross section. This approximation reproduces the correct leading order terms, which represent the strong and weak coupling case, respectively. Moreover, it is

a generalization of (3.11), that takes into account that the initial state is no longer the ground state so that $H_0 |i\rangle = E_i |i\rangle$. In our graphical representation, with respect to the $T = 0$ case, it corresponds to retain all the additional terms, having more than one kink, that start and finish with a horizontal step. In doing this, we are neglecting again the sub-leading order terms $H_c^{l-1-n} H_0 H_c^n$.

After inserting expansion (3.29) in the expression (3.3) for $M_l$, we finally have to evaluate

$$\langle f| \mathcal{D}^\dagger \sum_{n,m} (H_0)^m (H_c)^{l-m-n} (H_0)^n \mathcal{D} |i\rangle = \sum_{n,m} E_f^m E_i^n \langle f| \mathcal{D}^\dagger H_c^{l-m-n} \mathcal{D} |i\rangle . \quad (3.30)$$

In the local core hole approximation, we can resum this approximate series expansion. By using the results of Eqs. (3.17) and (3.18), we obtain for spinless fermions

$$M_l^{sf} = -\frac{1}{\Delta^l} \langle f| \rho_{\mathbf{q}} |i\rangle \sum_{n,m} E_f^m E_i^n U^{l-m-n}. \quad (3.31)$$

By performing the sums over $n$ and $m$

$$\sum_{n,m} E_f^m E_i^n U^{l-m-n} = U^l \sum_{n=0}^{l-1} (E_i/U)^n \sum_{m=0}^{l-n-1} (E_f/U)^m, \quad (3.32)$$

and after summing over $l$, we finally obtain

$$\mathcal{F}_{fi}^{sf} = P_1(E_f, U) \frac{\Delta}{\Delta - E_i} \langle f| \rho_{\mathbf{q}} |i\rangle . \quad (3.33)$$

This equation clearly shows that one of the main effects of finite temperature is to modify the resonant enhancement factor, nevertheless preserving the same structure for the scattering amplitude.

At this point we observe that at resonance $|\Delta| = \Gamma$, which is of the order of electronvolts and thus several orders of magnitude larger than $E_i$, even at high temperature. This allows us to approximate the prefactor in Eq. (3.33) as

$$P_1(E_f, U) \frac{\Delta}{\Delta - E_i} \approx P_1(\omega, U) \left(1 + \frac{E_i}{\Delta - \hbar\omega} + \dots\right) \left(1 + \frac{E_i}{\Delta} + \dots\right). \quad (3.34)$$

At the lowest order in $E_i/\Gamma$, the prefactor is not modified by $T$ at all, hence we conclude that the major modifications to the cross section are induced by thermal averaging of the correlation function. After integrating over all the incoming photon energies, we get the following approximate expression for the thermal average of the inelastic intensity at loss energy $\hbar\omega$ and momentum $\hbar\mathbf{q}$:

$$\left.\frac{d^2\sigma}{d\Omega d\omega}\right|_{\mathrm{res,T}} \propto |P_1(\omega)|^2 \langle S(\mathbf{q}, \omega)\rangle_{\mathrm{T}} . \quad (3.35)$$

In this expression the temperature dependence is entirely due to the temperature dependence of $S(\mathbf{q},\omega)$. The prefactor is in leading order temperature independent. Note that at finite temperatures also energy gain scattering occurs: the photon can gain an energy of the order of $k_BT$ from the system, which corresponds to a negative energy loss.

### 3.2.5 Fermions with spin

We generalize the calculation above to the situation where the electrons have an additional spin degree of freedom. In the Hamiltonians (3.5) and (3.6) we now include a spin index $\sigma$ (with $\sigma =\uparrow$ or $\downarrow$) to the annihilation and creation operators: $c_i \to c_{i\sigma}$ and $c_j \to c_{j\sigma'}$ and sum over these indices, taking into account that the hopping part of the Hamiltonian is diagonal in the spin variables. In order to resum the series in Eq. (3.11) we now need to evaluate expansions of the kind $(n_\uparrow + n_\downarrow)^l$ when we expand around the unscreened part of the resonant edge. Using

$$(n_\uparrow + n_\downarrow)^l = n_\uparrow + n_\downarrow + (2^l - 2)n_\uparrow n_\downarrow, \tag{3.36}$$

for $l > 0$, we obtain for the inelastic part

$$\mathcal{F}_{fi} = \langle f| \left(P_1(\omega,-U)[\rho_{\mathbf{q}} - 2\rho^{\uparrow\downarrow}_{\mathbf{q}}] + 2P_2(\omega,-U)\rho^{\uparrow\downarrow}_{\mathbf{q}}\right) |i\rangle\,, \tag{3.37}$$

with $P_2(\omega,U) = P_1(\omega,2U)/2$ and $\rho^{\uparrow\downarrow}_{\mathbf{q}} \equiv \sum_i e^{i\mathbf{q}\cdot\mathbf{R}_i} n_{i\uparrow}n_{i\downarrow}$. We see that in the case that each site can only be occupied by at most one valence electron, this equation reduces to Eq. (3.23) with $\rho_{\mathbf{q}} = \rho^{\uparrow}_{\mathbf{q}} + \rho^{\downarrow}_{\mathbf{q}}$. The two terms in the scattering amplitude can also be written in terms of density and spin operators. Using $(n_{i\uparrow} - n_{i\downarrow})^2 = (2S^z_i)^2 = \frac{4}{3}\mathbf{S}^2_i$, we obtain $\rho_{\mathbf{q}} - 2\rho^{\uparrow\downarrow}_{\mathbf{q}} = \mathbf{S}^2_{\mathbf{q}}$, where we introduce the longitudinal spin density correlation function $\mathbf{S}^2_{\mathbf{q}} \equiv \frac{1}{S(S+1)}\sum_{\mathbf{k}} \mathbf{S}_{\mathbf{k}+\mathbf{q}}\cdot\mathbf{S}_{-\mathbf{k}}$. In terms of these correlation functions the scattering amplitude for spinfull fermions is

$$\mathcal{F}_{fi} = [P_1(\omega,-U) - P_2(\omega,-U)]\,\langle f|\,\mathbf{S}^2_{\mathbf{q}}\,|i\rangle + P_2(\omega,-U)\,\langle f|\,\rho_{\mathbf{q}}\,|i\rangle\,, \tag{3.38}$$

Clearly the contributions to the scattering rate from the dynamic longitudinal spin correlation function and the density correlation function need to be treated on equal footing as they interfere. On a heuristic basis sometimes only the charge density response function is considered for the calculation of RIXS spectra, *e.g.*, [63–66]. Note that based on qualitative arguments, it was anticipated that the RIXS cross section should depend on a dynamic four-particle correlation function [38].

The spin and charge correlation functions have different resonant enhancements, see Fig. 3.2. For instance when $\mathfrak{Re}\{\Delta\} = -U$, the scattering amplitude is dominated by $P_1(\omega)$ and hence by the longitudinal spin response function. When the photons are tuned to the well-screened intermediate state on the other hand, *i.e.*, where $\mathfrak{Re}\{\Delta\} = -2U$, $P_2(\omega)$ is resonating so that the contributions to the inelastic scattering amplitude of charge and spin are approximately equal.

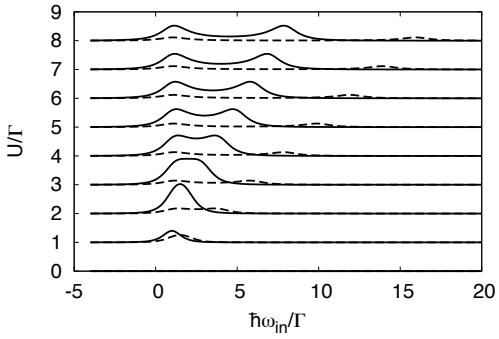


**Figure 3.2:** Prefactors to the scattering intensity at fixed loss energy ($\hbar\omega/\Gamma = 1$) as a function of incoming photon energy $\hbar\omega_{\text{in}}/\Gamma$, for different values of the local core hole potential $U/\Gamma$. The solid line refers to $|P_1(\omega, U)|^2$ and the dashed line refers to $|P_2(\omega, U)|^2$.

Again, these resonances are at energy-gain scattering. Alternatively, we can expand around the well-screened intermediate states. We then use the core hole Hamiltonian

$$H_c = U \sum_i s_i\, s_i^\dagger (2 - n_{i\uparrow} - n_{i\downarrow}) = U \sum_i s_i\, s_i^\dagger (c_{i\uparrow} c_{i\uparrow}^\dagger + c_{i\downarrow} c_{i\downarrow}^\dagger) \tag{3.39}$$

and obtain by an analogous procedure

$$\mathcal{F}_{fi} = [P_2(\omega, U) - P_1(\omega, U)] \langle f| \mathbf{S}_{\mathbf{q}}^2 |i\rangle + [3P_2(\omega, U) - 2P_1(\omega, U)] \langle f| \rho_{\mathbf{q}} |i\rangle . \tag{3.40}$$

In the case of the cuprates, the spinless fermion scenario is appropriate when considering charge scattering: the intra-ionic Coulomb repulsion is so large that the fermions will virtually never occupy the same site ($n_\uparrow n_\downarrow = 0$), which makes the spin degree of freedom irrelevant. In this limit $\mathbf{S}_{\mathbf{q}}^2 = \rho_{\mathbf{q}}$, and the scattering amplitudes for the spinless and spinfull fermions, expanded around the unscreened intermediate states – Eqs. (3.25) and (3.38) respectively – are equal. The well-screened intermediate states do not have an analogue in the spinless case, as no two fermions can occupy the same site to screen the core hole.

### 3.2.6 Multi-band systems

Let us consider systems with more than one band and take as an explicit example a transition metal with a 3d and a 4s band. The Coulomb attraction between the 1s core hole and an electron in the 3d state ($U_d$) is much larger than the interaction with a 4s electron ($U_s$). Neglecting spin degrees of freedom we would naively expect that the indirect RIXS response in the two-band system is simply the sum of the responses of the two individual electronic systems, with possible interference between the two scattering channels: we expect the scattering amplitude to be equal to

$$\mathcal{F}_{fi}^{s+d} = P_1(\omega, U_d) \langle f| \rho_{\mathbf{q}}^d |i\rangle + P_1(\omega, U_s) \langle f| \rho_{\mathbf{q}}^s |i\rangle . \tag{3.41}$$

However, already from the calculation for the spinfull fermions we know that the situation should be more complicated, as in that case the full response function is not just the sum of the two response functions for spinless fermions. The point is that when both a 3d and 4s electron screen the core hole, the intermediate state is at a lower energy (at $\hbar\omega_{\rm in} = U_d + U_s$) compared to the situation where only a single d or s electron screens the core hole (with a resonance at $\hbar\omega_{\rm in} = U_d$ or $U_s$, respectively.) In the situation that both electrons screen the core hole, the resonance therefore appears at a different incoming photon energy.

According to Eq. (3.15), we now need to evaluate expressions of the sort $(U_d n^d + U_s n^s)^l$ for $l > 0$ when expanding around the unscreened intermediate states. After using the binomial theorem and summing the resulting series, we obtain

$$(U_d n^d + U_s n^s)^l = U_d^l n^d + U_s^l n^s + n^d n^s \left[(U_d + U_s)^l - U_d^l - U_s^l\right], \tag{3.42}$$

which leads to a scattering amplitude

$$\mathcal{F}_{fi}^{sd} = \mathcal{F}_{fi}^{s+d} + \left[P_1(\omega, -U_d - U_s) - P_1(\omega, -U_d) - P_1(\omega, -U_s)\right] \langle f| \rho_{\mathbf{q}}^{ds} |i\rangle , \tag{3.43}$$

where $\rho_{\mathbf{q}}^{ds} \equiv \sum_i e^{i\mathbf{q}\cdot\mathbf{R}_i} n_i^d n_i^s$. This is an interesting term, physically, as it directly measures the density correlations between the d and s electron density on a transition metal atom.

Alternatively, we again expand around the well-screened intermediate states where both the d and s orbitals are occupied:

$$H_c = \sum_i c_i c_i^\dagger (U_d d_i d_i^\dagger + U_s s_i s_i^\dagger) \tag{3.44}$$

where $c_i$, $d_i$ and $s_i$ represent the core, d and s electron annihilation operators respectively. The corresponding scattering amplitude is

$$\begin{aligned}\mathcal{F}_{fi}^{sd} = &\left[P_1(\omega, U_d + U_s) - P_1(\omega, U_s)\right] \langle f| \rho_{\mathbf{q}}^{d} |i\rangle \\ &+ \left[P_1(\omega, U_d + U_s) - P_1(\omega, U_d)\right] \langle f| \rho_{\mathbf{q}}^{s} |i\rangle \\ &+ \left[P_1(\omega, U_d) + P_1(\omega, U_s) - P_1(\omega, U_d + U_s)\right] \langle f| \rho_{\mathbf{q}}^{ds} |i\rangle \end{aligned} \tag{3.45}$$

where $\rho_{\mathbf{q}}^{d,s} \equiv \sum_i e^{i\mathbf{q}\cdot\mathbf{R}_i} n_i^{d,s}$. Note that $\left[P_1(\omega, U_d + U_s) - P_1(\omega, U_s)\right] = 0$ when $U_d = 0$.

### 3.2.7 Conclusions

On the basis of the ultra-short lifetime of the core hole in the intermediate state we presented a series expansion of the indirect resonant inelastic X-ray scattering amplitude, which is asymptotically exact for both small and large local core hole potentials. This algebraic series is also given in a graphical representation. By resumming the terms in the series, we find the dynamical charge and spin

correlation functions that are measured in RIXS. The resonant prefactor is only weakly temperature dependent. We have also derived a sum rule for the total scattering intensity and considered RIXS in both single and multi-band systems. On the basis of our results, the charge and spin structure factor that is obtained from *ab initio* density functional calculations or from, *e.g.*, Hubbard-like model Hamiltonians can directly be compared to experimental RIXS spectra. Moreover, our results open up the possibility to compare the measurements of $S(\mathbf{q},\omega)$ by RIXS and, for instance, electron energy loss spectroscopy [67]. In this way one can actually determine experimentally the resonant scattering prefactors that we have calculated.

We should stress that four basic assumptions underly our results, which otherwise are general. First, the RIXS process that we consider is *indirect*, *i.e.*, in the scattering process electrons are *not* directly promoted into the conduction band of the solid. Rather the inelastic scattering that we consider is due to the potential of the core hole which is present in the intermediate state. This situation arises, for instance, at the K edge of transition metal atoms, but can also occur at the L edge of lanthanide ions. We assumed, furthermore, that the core hole is localized and that its lifetime is short – reasonable premises for the deep core holes that are involved. The final assumption is that scattering is dominated by the coupling between the core hole and electrons (of d character if we consider a transition metal K edge) *on the same atom*. This is a good approximation when the d electrons are localized and the on-site Coulomb interaction is much larger than the one between neighboring atoms. In that sense our ultra-short lifetime expansion is expected to work very well for 3d systems and possibly less so for the 4d or 5d transition metal ions.

Finally, we assumed that the charge and longitudinal spin responses of the system that we consider are not vanishing, *i.e.*, they are the leading order response function. In insulators at energies below the gap, however, these two response functions do vanish. This in principle opens a way to observe correlation functions beyond the ones that we have considered here, for instance, transversal spin (chapter 4) or orbital response functions (chapter 5) and thus to measure magnon dispersions or even orbiton properties with RIXS – a very exciting prospect indeed.

### 3.2.8 Acknowledgments

We thank Michel van Veenendaal and John P. Hill for stimulating our interest in the theory of indirect resonant inelastic X-ray scattering, for intense discussions, for critical reading of the manuscript and for their generous hospitality. We thank Stephane Grenier, Young-June Kim, Philip Platzman and George Sawatzky for fruitful discussions. We gratefully acknowledge support from the Argonne National Laboratory Theory Institute, Brookhaven National Laboratory (DE-AC02-98CH10996), and the Dutch Science Foundation FOM.

## 3.3 Corrections to the cross section for strong core hole potentials

In this section we consider the first order correction to the UCL results given in Sec. 3.2. We treat the cases of spinless fermions (Sec. 3.3.1) and fermions with spin (Sec. 3.3.2) in the limit of a strong core hole potential. The resulting correction terms to the RIXS scattering amplitude contain information on the hopping matrix elements.

### 3.3.1 Spinless fermions

In Sec. 3.2, $H_{\text{int}}^l$ was approximated in the limit of a strong core hole potential as $(H_0 + H_c)^l \approx H_c^l$. The first order correction to this approximation has one factor of $H_0$ and $l-1$ factors of $H_c$, and those terms are not properly included in the UCL expansion for $l \geq 2$. We therefore improve the approximation:

$$(H_0 + H_c)^l = H_c^l + \sum_{n=0}^{l-2} H_c^n H_0 H_c^{l-1-n} + \mathcal{O}(H_0^2) \tag{3.46}$$

for $l > 2$. The $l \leq 2$ terms were exact already in Sec. 3.2. The $n = 0$ term was also already included. The first order corrections to Eq. (3.2) for spinless fermions are therefore of the form

$$\langle f| \mathcal{D}^\dagger \sum_{n=1}^{l-2} H_c^n H_0 H_c^{l-1-n} \mathcal{D} |i\rangle = U^{l-1}(l-2) \langle f| \sum_i e^{i\mathbf{q}\cdot\mathbf{R}_i} c_i c_i^\dagger H_0 c_i c_i^\dagger |i\rangle \tag{3.47}$$

when expanding around the well-screened intermediate states.

Now we commute $H_0$ to the right:

$$\left[H_0, c_i c_i^\dagger\right] = \sum_j t_{ij} \left(c_i^\dagger c_j - c_j^\dagger c_i\right). \tag{3.48}$$

where we assumed $t_{ij}$ and $t_{ji}$ are equal and real numbers. The correction terms (3.47) then become

$$\langle f| \mathcal{D}^\dagger \sum_{n=1}^{l-2} H_c^n H_0 H_c^{l-1-n} \mathcal{D} |i\rangle = -U^{l-1}(l-2) \langle f| \sum_{i,j} e^{i\mathbf{q}\cdot\mathbf{R}_i} t_{ij} c_j^\dagger c_i |i\rangle . \tag{3.49}$$

Fourier transforming gives

$$\langle f| \mathcal{D}^\dagger \sum_{n=1}^{l-2} H_c^n H_0 H_c^{l-1-n} \mathcal{D} |i\rangle = -U^{l-1}(l-2) \langle f| \sum_{\mathbf{k}} t_{\mathbf{k}} c_{\mathbf{k}}^\dagger c_{\mathbf{k}-\mathbf{q}} |i\rangle , \tag{3.50}$$

where the $t_{\mathbf{k}} = \sum_i t_{i0} e^{-i\mathbf{k}\cdot\mathbf{R}_i}$ are the Fourier components of $t_{ij}$, assuming $t_{ij}$ to be invariant under translations.

The inelastic scattering amplitude becomes

$$\mathcal{F}_{fi} = \frac{1}{\Delta}\sum_{l=1}^{\infty}\frac{1}{\Delta^l}\langle f|\,\mathcal{D}^\dagger(H_0+H_c)^l\mathcal{D}\,|i\rangle \tag{3.51}$$

$$\approx P_1\langle f|\,\rho_{\mathbf{q}}\,|i\rangle - \frac{U}{\Delta^3}\sum_{l=2}^{\infty}\left(\frac{U}{\Delta}\right)^{l-2}(l-2)\langle f|\sum_{\mathbf{k}} t_{\mathbf{k}}c^\dagger_{\mathbf{k}}c_{\mathbf{k}-\mathbf{q}}\,|i\rangle \tag{3.52}$$

$$= P_1\langle f|\,\rho_{\mathbf{q}}\,|i\rangle + P_3\langle f|\sum_{\mathbf{k}} t_{\mathbf{k}}c^\dagger_{\mathbf{k}}c_{\mathbf{k}-\mathbf{q}}\,|i\rangle \tag{3.53}$$

with $P_3 = -\frac{U^2}{\Delta^2(\Delta-U)^2}$. The correction terms carry information about the hopping matrix elements $t_{ij}$. They involve two-site correlation functions. Higher order correction terms can generate correlation functions with more and more sites. Especially for systems with only a single fermion, or at least very few fermions, that are at a fixed momentum, RIXS is able to directly probe the hopping matrix elements. It should be noted, however, that the $P_1$ and $P_3$ terms of the scattering amplitude interfere, and that this interference term is of order $t_{ij}/\Delta$ stronger than the $|P_3|^2$ term.

### 3.3.2 Fermions with spin 1/2

When the fermions have a spin index, we have to evaluate for $l > 2$:

$$\begin{aligned}
&\langle f|\,\mathcal{D}^\dagger\sum_{n=1}^{l-2}H_c^nH_0H_c^{l-1-n}\mathcal{D}\,|i\rangle \\
&= U^{l-1}\sum_{n=1}^{l-2}\langle f|\sum_i e^{i\mathbf{q}\cdot\mathbf{R}_i}\left(\sum_\sigma c_{i\sigma}c^\dagger_{i\sigma}\right)^n H_0\left(\sum_{\sigma'}c_{i\sigma'}c^\dagger_{i\sigma'}\right)^{l-1-n}|i\rangle \\
&= U^{l-1}\sum_{n=1}^{l-2}\langle f|\sum_i e^{i\mathbf{q}\cdot\mathbf{R}_i}\left(c_{i\uparrow}c^\dagger_{i\uparrow}+c_{i\downarrow}c^\dagger_{i\downarrow}+(2^n-2)c_{i\uparrow}c^\dagger_{i\uparrow}c_{i\downarrow}c^\dagger_{i\downarrow}\right)\times \\
&\quad H_0\left(c_{i\uparrow}c^\dagger_{i\uparrow}+c_{i\downarrow}c^\dagger_{i\downarrow}+(2^{l-1-n}-2)c_{i\uparrow}c^\dagger_{i\uparrow}c_{i\downarrow}c^\dagger_{i\downarrow}\right)|i\rangle\,.
\end{aligned} \tag{3.54}$$

$H_0$ is commuted to the right:

$$\begin{aligned}
&\left[H_0,\left(c_{i\uparrow}c^\dagger_{i\uparrow}+c_{i\downarrow}c^\dagger_{i\downarrow}+(2^{l-1-n}-2)c_{i\uparrow}c^\dagger_{i\uparrow}c_{i\downarrow}c^\dagger_{i\downarrow}\right)\right] = \sum_{j,\sigma}t_{ij}\left(c^\dagger_{i\sigma}c_{j\sigma}-c^\dagger_{j\sigma}c_{i\sigma}\right) \\
&+(2^{l-1-n}-2)\left(\left[H_0,c_{i\uparrow}c^\dagger_{i\uparrow}\right]c_{i\downarrow}c^\dagger_{i\downarrow}+c_{i\uparrow}c^\dagger_{i\uparrow}\left[H_0,c_{i\downarrow}c^\dagger_{i\downarrow}\right]\right) \\
&=\sum_{j,\sigma}t_{ij}\left(c^\dagger_{i\sigma}c_{j\sigma}-c^\dagger_{j\sigma}c_{i\sigma}\right)\left(2^{l-1-n}-1+(2^{l-1-n}-2)n_{i\bar\sigma}\right),
\end{aligned} \tag{3.55}$$

where $\bar{\sigma} = \uparrow$ if $\sigma = \downarrow$, and vice versa. We find after some algebra

$$\begin{aligned}
&\langle f|\,\mathcal{D}^\dagger \sum_{n=1}^{l-2} H_c^n H_0 H_c^{l-1-n} \mathcal{D}\,|i\rangle \\
&\quad = U^{l-1} \sum_{i,j,\sigma} e^{i\mathbf{q}\cdot\mathbf{R}_i} t_{ij} \,\langle f|\,\Big[ -(l-2)\, c^\dagger_{j\sigma} c_{i\sigma} - \big((l-3)2^{l-1} + 4 - l\big)\, c_{i\bar{\sigma}} c^\dagger_{i\bar{\sigma}} c^\dagger_{j\sigma} c_{i\sigma} \\
&\qquad + \big(2^{l-1} - l\big)\, c_{i\bar{\sigma}} c^\dagger_{i\bar{\sigma}} c^\dagger_{i\sigma} c_{j\sigma} \Big]\,|i\rangle\,. \qquad (3.56)
\end{aligned}$$

The inelastic scattering amplitude $\mathcal{F}_{fi}$ is then

$$\begin{aligned}
\mathcal{F}_{fi} &= \frac{1}{\Delta} \sum_{l=1}^{\infty} \frac{1}{\Delta^l} \,\langle f|\,\mathcal{D}^\dagger (H_0 + H_c)^l \mathcal{D}\,|i\rangle \qquad (3.57) \\
&\approx (\text{uncorrected terms}) + P_3 \sum_{i,j,\sigma} t_{ij} e^{i\mathbf{q}\cdot\mathbf{R}_i} \,\langle f|\,\Big[ c^\dagger_{j\sigma} c_{i\sigma} \\
&\quad - \frac{\Delta}{\Delta - 2U} c_{i\bar{\sigma}} c^\dagger_{i\bar{\sigma}} c^\dagger_{i\sigma} c_{j\sigma} + \frac{\Delta^2 + 2U\Delta - 4U^2}{(\Delta - 2U)^2} c_{i\bar{\sigma}} c^\dagger_{i\bar{\sigma}} c^\dagger_{j\sigma} c_{i\sigma} \Big]\,|i\rangle\,, \qquad (3.58)
\end{aligned}$$

where "uncorrected terms" refers to Eq. (3.40).

For the special case of a half-filled system without doubly occupied sites in the initial state, the scattering amplitude is

$$\mathcal{F}_{fi} = (\text{uncorr.}) + P_3 \sum_{\mathbf{k},\sigma} \left[ \frac{2\Delta(\Delta - U)}{(\Delta - 2U)^2} t_{\mathbf{k}+\mathbf{q}} - \frac{\Delta}{\Delta - 2U} t_{\mathbf{k}} \right] \langle f|\, c^\dagger_{\mathbf{k}+\mathbf{q},\sigma} c_{\mathbf{k}\sigma}\,|i\rangle\,. \qquad (3.59)$$

## 3.4 Polarization dependence of transition metal K edge RIXS

In Sec. 3.2, the polarization details of the indirect RIXS scattering process at the transition metal K edge were neglected: all $T(\boldsymbol{\epsilon}', \boldsymbol{\epsilon})$ were set to 1. In this section, the polarization dependence of the two dipole transitions is investigated in more detail. The previous results is modified by a polarization-dependent prefactor $T(\boldsymbol{\epsilon}', \boldsymbol{\epsilon})$.

In the following, it is assumed that the 4p electron acts as a spectator, that is, different 4p states do not give rise to different scattering processes [4, 5]. These are determined by the 1s core hole alone.

In an octahedral crystal feld, the polarization dependence of indirect RIXS at the transition metal K edge might at first sight seem trivial: excitation of a 1s core electron into a 4p level and the consecutive de-excitation yields the

polarization dependence (2.42)

$$T(\boldsymbol{\epsilon}',\boldsymbol{\epsilon}) = \sum_i \langle 1s|\, \boldsymbol{\epsilon}'^* \cdot \mathbf{r}\, |4p_i\rangle \langle 4p_i|\, \boldsymbol{\epsilon}\cdot\mathbf{r}\, |1s\rangle \propto \sum_{i,n,m} \iint d\mathbf{r}d\mathbf{r}'\ \epsilon'^*_n r'_n r'_i r_i \epsilon_m r_m$$
$$\propto \sum_{i,n,m} \epsilon'^*_n \delta_{n,i}\delta_{i,m}\epsilon_m = \boldsymbol{\epsilon}'^*\cdot\boldsymbol{\epsilon}. \tag{3.60}$$

Deviations from octahedral symmetry induce an anisotropy. In $La_2CuO_4$, for instance, the $4p_z$ state is at a slightly different energy than the $4p_{x,y}$ because of the planar structure of the material. In the extreme case that the off-resonant $4p_z$ states do not contribute at all to the RIXS scattering amplitude, $T(\boldsymbol{\epsilon}',\boldsymbol{\epsilon}) = \epsilon'^*_x\epsilon_x + \epsilon'^*_y\epsilon_y$.

Apart from these local effects, however, there is another important anisotropic contribution to the polarization dependence. The 4p states form bands, and the $4p_x$ and $4p_y$ orbitals can mix. We now show the effect of this mixing in a minimal model for the 4p states. Nearest neighbor 4p orbitals only have non-zero hopping from $4p_x$ to $4p_x$ and from $4p_y$ to $4p_y$. Next-nearest neighbor hopping is substantial because of the extended nature of the 4p states. This can couple $4p_x$ and $4p_y$ orbitals, and we only include this part of the next-nearest neighbor hopping in the Hamiltonian:

$$H = -t\sum_{i,\delta}\left(p^\dagger_{x,i}p_{x,i+\delta} + p^\dagger_{y,i}p_{y,i+\delta}\right) - t'\sum_{i,\delta'}\left(p^\dagger_{y,i}p_{x,i+\delta'} + p^\dagger_{x,i}p_{y,i+\delta'}\right) \tag{3.61}$$

where $p_{x,y}$ annihilates an electron in the $4p_{x,y}$ orbital. $t$ is the nearest neighbor hopping amplitude, which is assumed to be equal in all directions for simplicity, and $t'$ is the hopping amplitude for next-nearest neighbors. $\delta$ and $\delta'$ point to nearest and next-nearest neighbors, respectively. This Hamiltonian is easily diagonalized in $\mathbf{k}$ space:

$$H = \sum_{\mathbf{k}}\left[\left(-zt\gamma_{\mathbf{k}} + z't'\gamma'_{\mathbf{k}}\right)\alpha^\dagger_{\mathbf{k}}\alpha_{\mathbf{k}} + \left(-zt\gamma_{\mathbf{k}} - z't'\gamma'_{\mathbf{k}}\right)\beta^\dagger_{\mathbf{k}}\beta_{\mathbf{k}}\right] \tag{3.62}$$

where $\gamma_{\mathbf{k}}(') = \sum_{\delta(')} e^{i\mathbf{k}\cdot\boldsymbol{\delta}(')}/z(')$ with $z$ the number of nearest neighbors and $z'$ the number of next-nearest neighbors. We introduced transformed fermion operators $\alpha_{\mathbf{k}}$ and $\beta_{\mathbf{k}}$:

$$\begin{pmatrix} p_{x,\mathbf{k}} \\ p_{y,\mathbf{k}}\end{pmatrix} = \frac{1}{\sqrt{2}}\begin{pmatrix} 1 & 1 \\ -1 & 1\end{pmatrix}\begin{pmatrix}\alpha_{\mathbf{k}} \\ \beta_{\mathbf{k}}\end{pmatrix}. \tag{3.63}$$

Within this model, the polarization factors (2.42) are

$$T_\alpha(\boldsymbol{\epsilon}',\boldsymbol{\epsilon}) = \langle 1s|\, \boldsymbol{\epsilon}'^*\cdot\mathbf{r}\, |\alpha_{\mathbf{k}}\rangle\langle\alpha_{\mathbf{k}}|\, \boldsymbol{\epsilon}\cdot\mathbf{r}\, |1s\rangle \propto \iint d\mathbf{r}d\mathbf{r}'\ \boldsymbol{\epsilon}'^*\cdot\mathbf{r}'(x'-y')(x-y)\boldsymbol{\epsilon}\cdot\mathbf{r}$$
$$\propto (\epsilon'^*_x - \epsilon'^*_y)(\epsilon_x - \epsilon_y), \tag{3.64}$$

$$T_\beta(\boldsymbol{\epsilon}', \boldsymbol{\epsilon}) = \langle 1s| \boldsymbol{\epsilon}'^* \cdot \mathbf{r} |\beta_\mathbf{k}\rangle \langle \beta_\mathbf{k}| \boldsymbol{\epsilon} \cdot \mathbf{r} |1s\rangle \propto \iint d\mathbf{r} d\mathbf{r}' \ \boldsymbol{\epsilon}'^* \cdot \mathbf{r}'(x' + y')(x + y)\boldsymbol{\epsilon} \cdot \mathbf{r}$$
$$\propto (\epsilon_x'^* + \epsilon_y'^*)(\epsilon_x + \epsilon_y). \tag{3.65}$$

The $4p_z$ states will contribute a term proportional to $\epsilon_z'^* \epsilon_z$. When $t' = 0$, $|\alpha_\mathbf{k}\rangle$ and $|\beta_\mathbf{k}\rangle$ are degenerate and we recover the result for atomic 4p states: $T_\alpha + T_\beta \propto \boldsymbol{\epsilon}'^* \cdot \boldsymbol{\epsilon}$. However, when next-nearest neighbor hopping is non-zero, the degeneracy of the 4p states is lifted. When this splitting becomes of the order of $\Gamma$, the energy denominator in Eq. (2.41) becomes appreciably different and the polarization dependences of $T_\alpha$ and $T_\beta$ no longer add with equal weight.

In our simple model, the hopping $t'$ introduces a mixing of $4p_x$ and $4p_y$ orbitals, which of course can also be introduced in other ways, like spin-orbit coupling, scattering off the valence electrons, etc. In general, all these effects, together with the deviations from the cubic crystal field mentioned above, will produce an anisotropic polarization dependence.

## 3.5 Comparison to experiments

The observation that within the UCL the RIXS cross section can be factored into a resonant prefactor and the dynamic structure factor $S(\mathbf{q}, \omega)$, was tested experimentally by Kim *et al.* [67]. They reported an empirical comparison of Cu K edge indirect RIXS spectra, taken at the Brillouin zone center, with optical dielectric loss functions measured in a number of copper oxides: $Bi_2CuO_4$, $CuGeO_3$, $Sr_2Cu_3O_4Cl_2$, $La_2CuO_4$, and $Sr_2CuO_2Cl_2$. Analyzing both incident and scattered photon resonances, they extracted a response function that is independent of the incident energy. The overall spectral features of the indirect RIXS spectral function were found to be in reasonable agreement with the optical dielectric loss function over a wide energy range. In the case of $Bi_2CuO_4$ and $CuGeO_3$, Ref. [67] observes that the incident energy-independent response function, $S(\mathbf{q} = \mathbf{0}, \omega)$, matches very well with the dielectric loss function, $-\Im\mathfrak{m}\{1/\epsilon(\omega)\}$ measured with spectroscopic ellipsometry, suggesting that the local core hole approximation treatment of the UCL works well in these more localized electron systems. Corner sharing two-dimensional copper oxides exhibit more complex excitation features than observed in the dielectric loss functions, likely related to non-local core hole screening effects.